Astron. Astrophys. 340, 476–482 (1998)

ASTRONOMY
AND
ASTROPHYSICS

Spectral analysis of the low-gravity extreme helium stars LSS 4357, LS II+33 °5 and LSS 99⋆

C.S. Jeffery[1], **Peter J. Hamill**[1], **Paul M. Harrison**[1], **and Sandra V. Jeffers**[1]

Armagh Observatory, College Hill, Armagh BT61 9DG, UK

Received 19 May 1998 / Accepted 25 September 1998

Abstract. We have carried out quantitative analyses of three very low surface gravity extreme helium stars with very similar spectra. Their effective temperatures of $\sim 16\,000$K fill a gap in a nearly continuous sequence of extreme helium stars all having similar luminosity-to-mass ratios, but extending from effective temperatures around 12 000 K to more than 20 000 K. Because of the low surface gravities and extremely rich line spectra, the model atmosphere calculations have been reviewed, and large-scale spectral synthesis techniques have been introduced to the analyses for the first time. In addition to the high carbon and nitrogen abundances usually seen in extreme helium stars, two of the programme stars have extremely high oxygen abundances, comparable with or greater than their carbon abundances.

Key words: stars: individual: (LS II+33 °5, LSS 4357, LSS 99) – stars: emission-line, be – stars: chemically peculiar – stars: abundances

1. Introduction

The group of extreme helium stars (EHes) at present comprises some 20 objects. These stars have early-type spectra dominated by strong neutral helium, singly-ionized carbon and almost undetectable Balmer lines. Most show high luminosity-to-mass ratios. Indicators such as galactic location and pulsation point to masses in the range 0.7 to 1.0 $M_\odot$. Their surface gravities imply luminosities typical of post-asymptotic giant branch stars ($10^3 - 10^4 L_\odot$). The question posed is how they come to have typical photospheric hydrogen abundances of less than one part in 10^4 or, in other words, what is their evolutionary status?

Previous studies of surface abundances in extreme helium stars (Jeffery 1996) have demonstrated that, in addition to hydrogen, their photospheres show anomalous proportions of carbon, nitrogen and oxygen, and other elements. These are indicative that in general the surface helium is the product of CNO cycling, and that there is a significant contamination by material that has been converted to carbon and possibly oxygen by $\alpha-$burning processes. The origin of other abundance anomalies, including those of neon and phosphorous remains undetermined.

The simultaneous presence of traces of primordial stellar material and CNO- and 3α- processed waste in the stellar photosphere points to a history that includes considerable mixing between layers of a highly evolved star. The principle hypotheses proposed to explain this mixing involve either a late helium flash in a cooling white dwarf or the coalescence of a helium and carbon-oxygen white dwarf. More precisely, these are the late thermal pulse (LTP) model of Iben et al. (1983) or the very late thermal pulse (VLTP) model of Blöcker & Schönberner (1997) and the merged binary white dwarf (MBWD) model of Webbink (1984) and Iben & Tutukov (1985).

The question of the origin of the extreme helium stars is closely related to that of the R Coronae Borealis stars. These cooler stars have photospheric abundances very similar to those of the extreme helium stars, although the carbon abundance has proved difficult to establish (Asplund 1997). A major study of abundances in these objects (Lambert et al. 1997) prefers the LTP model as origin.

Although a general picture of the photospheric abundances in helium stars can be given in a few sentences, individual stars show large deviations from the mean (Jeffery 1996). Thus their evolutionary origin (or origins) must be capable of generating a wide range of outcomes. A study of abundances in extreme helium stars has been in progress for several years in an effort to delimit this range and analyses of some ten EHes have been completed. This study presents results for the remaining EHes with effective temperatures between 14 000 and 30 000 K.

The extreme helium stars LSS 4357, LS II+33 °5 and LSS 99 were all discovered by Drilling during his surveys of OB+ stars in the Milky Way (Drilling & Hill 1986, Vijapurkar & Drilling 1993). A preliminary analysis of these stars was made by Heber et al. (1986), together with the extreme helium star LSE 78, who concluded that their effective temperatures were in the range 14 000 to 20 000 K and that their surface gravities were lower than covered by their grid of LTE model atmospheres. This study refines that earlier conclusion by applying the method of fine analysis to high resolution optical spectra. As a consequence of the rich absorption line content of these spectra, conventional line-by-line techniques have been superceded by large-scale spectral synthesis methods introduced here.

Send offprint requests to: C.S. Jeffery (csj@star.arm.ac.uk)

⋆ Based on observations obtained at the European Southern Observatory, La Silla, Chile.

These analyses provide abundance measurements for most of the astrophysically important light elements and are consistent with previous studies of other extreme helium stars. Together with work on four cooler helium stars nearing completion (Pandey et al., in preparation), this contribution will establish a comprehensive picture of the abundances in helium stars and will be reviewed in a concluding paper.

2. Observations

Blue-visual spectra of the program stars were obtained by U. Heber using CASPEC, a Cassegrain échelle spectrograph, on the ESO 3.6m telescope at La Silla, Chile, on 1984 April 4, 1985 April 5 and 8, and 1987 April 18. The data reduction has been described by Heber et al. (1986) and by Jeffery & Heber (1992), and yields a single wavelength calibrated spectrum corrected for the blaze function in each échelle order.

In general, observations of stellar spectra are affected by photon noise, wavelength calibration errors, instrumental calibration errors, cosmic ray events and non-stellar spectral features. These may introduce many problems when fitting a large section of synthetic spectrum ($\sim$ 1000Å) in order to analyse many lines simultaneously.

To ensure that the wavelength registration was correct, a synthetic spectrum of approximately the correct effective temperature, gravity and composition was constructed. The velocity shift between the observed and synthetic spectra was measured by cross-correlation, and the wavelengths in the observed spectrum were then shifted to the laboratory rest frame. This global velocity correction did not correct for local calibration errors, in individual échelle orders for example, which became apparent during the subsequent analysis. However, integrated over the entire spectrum, their nett contribution is stochastic rather than systematic.

The reconstruction of the stellar spectrum from several overlapping orders of an échellogram in which the blaze correction is difficult to calibrate is another major source of error. The problem is too identify the continuum correctly without compromising the wings of broad absorprion lines, especially those of He I. The original normalization of the CASPEC spectrum was carried out by attempting to correct each échelle order for the convolution of the order blaze function and the local stellar continuum. Whilst adequate over small sections of spectrum, the overall result is not satisfactory in the current sample. A procedure has been applied which re-normalizes the spectra in an objective fashion using regions of spectrum dominated by continuum. Further details are given in an appendix.

3. Model atmospheres

The surface gravities of the programme stars were known to be low (Heber et al. 1986), placing their atmospheres close to the Eddington limit. As has been usual for our studies of extreme helium stars, a large number of model atmospheres had to be calculated in order to analyse their surface abundances. It quickly became apparent that the ionization equilibria predicted by these models were almost independent of effective temperature, and so considerable effort was spent on verifying the models.

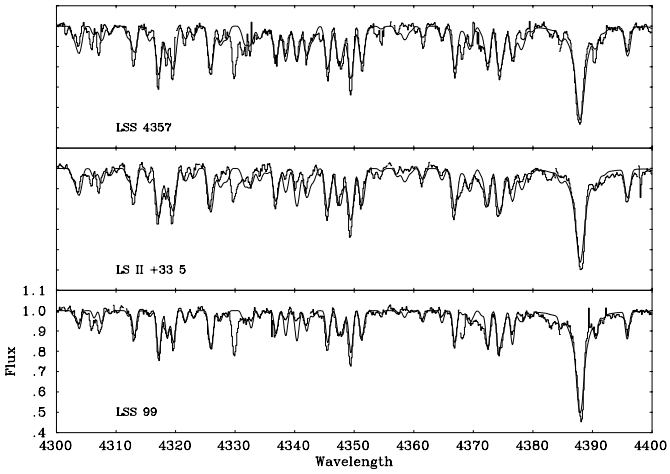

Fig. 1. Sections of the normalized CASPEC spectra of three helium stars LSS 4357, LS II+33 5 and LSS 99 are shown (histogram) together with synthetic spectra (smooth curve) calculated using the photospheric parameters and abundances given in Tables 1 and 2. Gaps indicate where cosmic ray hits have been removed; a few remain.

A well-known feature of hydrogen-deficient model atmospheres at low surface gravity is their poor convergence properties. As implemented, the model atmosphere code STERNE solved the radiative transfer equations using the scheme originally proposed by Avrett & Loeser (1963), and calculated the temperature correction following the Lucy-Unsöld procedure (Lucy 1964), accelerated according to the method proposed by Ng (1974). Due to computational time considerations, convergence has customarily been accepted when the mean square relative temperature correction has fallen below some value, normally $\langle \delta T^2/T \rangle \leq 0.003$. This is usually achieved after 40 iterations of the code. It was believed that the Avrett-Loeser solution of the transfer equation may be prone to instabilities, particularly at very small optical depths, so it has been replaced by a Feautrier scheme (Feautrier 1964). At present this assumes coherent scattering, although partial and complete redistribution can also be treated. It was also found that the Ng acclerator did not have a major effect on the convergence, indeed it was prone to delay convergence and was switched off. Other pertinent features of STERNE were described by Jeffery & Heber (1992). Line-blanketing is treated through fixed composition opacity distribution functions calculated for a hydrogen-deficient mixture by Möller (1990).

With these changes, convergence was found to be excellent at optical depths $\tau_{4000} > 10^{-2}$ where the temperature corrections converged to zero within approximately 30 iterations. However at small optical depths, the corrections remain significant and always negative. After many iterations, their amplitude decreases, but never reaches zero or changes sign. The effect is that the temperature of the outermost layers of the model at-

Table 1. Final parameters for low-gravity EHes

	LSS 4357	LS II+33°5	LSS 99	LSE 78 Jeffery 1993	DY Cen Jeffery & Heber 1993
$T_{\rm eff}$ (K)	$16\,130 \pm 500$	$16\,180 \pm 500$	$15\,330 \pm 500$	18 000	19 500
$\log g$ (cgs)	2.00 ± 0.25	2.00 ± 0.25	1.90 ± 0.25	2.00	2.15
$v_{\rm t}$ (km/s)	15 ± 5	15 ± 5	15 ± 5	20	20
$v \sin i$ (km/s)	45 ± 5	45 ± 5	30 ± 5	≤ 20	≤ 20

Table 2. Atmospheric abundances of three low-gravity EHes compared with other EHe and R CrB stars. Abundances are given (i) as $\log n$, normalised to $\log \Sigma \mu n = 12.15$ and (ii) as $[X/Fe] \equiv \log(\,n_{\rm X}/\,n_{\rm Fe})_\star - \log(\,n_{\rm X}/\,n_{\rm Fe})_\odot$, where the values adopted for [Fe] is shown in the final column.

Star	H	He	C	N	O	Mg	Al	Si	P	S	A	Ca	Fe	Ref.
(i) $\log n$														
LSS 4357	8.3	11.5	9.38	8.16	9.39	7.58	5.94	8.00	5.65	7.12	6.31	6.16	6.84	
LSS II+33°5	8.4	11.5	9.39	8.16	9.37	7.55	5.94	7.54	5.64	7.10	6.27	6.13	6.80	
LSS 99	8.0	11.5	9.13	7.61	8.59	7.55	5.67	7.31	5.22	6.92	6.23	6.17	6.89	
Sun	12.0	11.0	8.6	8.1	8.9	7.6	6.5	7.6	5.5	7.2	6.6	6.4	7.5	1
(ii) [X/Fe]														[Fe]
LSS 4357	-3.5		1.12	0.41	0.76	0.30	-0.23	0.75	0.45	0.22	0.01	0.06	-0.36	-0.3
LSS II+33°5	-3.3		1.13	0.41	0.74	0.27	-0.23	0.29	0.44	0.20	-0.03	0.03	-0.40	-0.3
LSS 99	-3.7		0.87	-0.14	-0.04	0.27	-0.50	0.06	0.02	0.02	-0.07	0.07	-0.31	-0.3
EHes (1)	-3.5		1.4	1.0	0.0	0.5	0.3	0.4	1.0	0.5				2
RCrBs (2)	-5.4		1.3	1.6	0.3	0.8	0.5	0.6	(1.5)	0.7				3

Notes.
() value from one star.
Means include the following stars. (1) HD16876, BD+10°2179, BD−9°4395, HD124448, LSE 78, LSS 3184. (2) R CrB, RY Sgr, XX Cam, SU Tau, UX Ant, UV Cas, UW Cen, V482 Cyg, Y Mus, RT Nor, RZ Nor, FH Sct, GU Sgr, RS Tel. [C/Fe] is uncertain because C I is the principal opacity source in helium stars with $T_{\rm eff} \lesssim 10\,000$K.

References. 1: Grevesse et al. 1996, 2: Jeffery 1996, 3:-Asplund 1997, Lambert et al. 1997.

mosphere decreases asymptotically. Even after 300 iterations, $|\delta T| > 1$K, for $\tau < 10^{-4}$.

Possible causes for the poor convergence were investigated. Although changing a boundary condition changes the final model, it does not alter the convergence behaviour. The omission of line blanketing allows the models to converge more rapidly and successfully with $\langle \delta T^2/T \rangle \leq 10^{-4}$. Our conclusion is that the use of the Lucy-Unsöld temperature-correction procedure is at fault. Temperature correction procedures leave the temperature structure of the outermost layers essentially undetermined particularly when the radiation field is only weakly coupled to the local thermal pool, as is the case here where scattering dominates (see Mihalas 1978, p175). A resolution awaits the implementation of a more sophisticated correction procedure.

Since most of the model atmosphere, including the region where most of the spectral lines are formed, has converged successfully, it remained likely that these models could be used for our analyses. Synthetic spectra including lines formed at a large range of optical depths were calculated, using models converged after 50, 100 and 300 iterations. The absence of convergence at small optical depths had no effect on these spectra, apart from the cores of very strong lines, including He I, Si III$_1$, and C II λ4267 Å. All of these lines were already known to show discrepancies between theory and observation which have been previously attributed to departures from local thermal equilibrium (LTE) (Heber 1983, Jeffery & Heber 1992). The current result suggests that at least part of the resolution will be achieved by constructing model atmospheres for low-gravity helium stars which are fully self-consistent at small optical depths.

The present study relies on the dual approximations of plane-parallel geometry and local thermodynamic equilibrium; departures from both become increasingly important in the atmospheres of low gravity stars. The atmospheres of the current sample are only "slightly extended" according to the definition of Schmid-Burgk & Scholz (1975). The latter found that, for the low-gravity halo star Barnard 29, the differences between plane parallel and spherical model atmospheres amounted to a few per cent in the upper atmosphere. However they doubted that abundance discrepancies relative to γ Peg could be explained by extended atmosphere effects. A similar argument applies here. We do not observe any other phenomena associated with extended atmospheres in the current sample. For example, there is no evidence of emission lines, such as those observed in the low-gravity helium stars DY Cen (Jeffery & Heber 1993) and

BD$-9^\circ 4395$ (Jeffery & Heber 1992) and which have been attributed to a circumstellar shell.

The approximation of local thermodynamic equilibrium is frequently violated in low gravity stars, with the combined effects of modifying both the global structure of the atmosphere and the profiles of individual absorption lines. The correct approach is to calculate both model atmospheres and synthetic spectra without this approximation. To date, the only successful attempt to compute NLTE spectra for non-expanding low-gravity hydrogen-deficient model atmospheres with $T_{\rm eff} \lesssim 40\,000$K found extremely slow convergence in a model containing only H, He and C (Rauch 1996). At lower temperatures, the neglect of line blanketing caused by the omission of other species will have consequences for the global structure of the atmosphere which are far more profound than the LTE approximation (Dudley & Jeffery 1993, Anderson & Grigsby 1991).

Until the problem of non-LTE model atmospheres has been solved, line-blanketed plane-parallel LTE models remain the most appropriate (and only) choice for the analysis of the present sample. This is not a poor choice, since it allows us to make a direct comparison with other extreme helium stars (and also RCrB stars, Asplund 1997) analyzed using similar methods; many of these have L/M ratios similar to or higher than the present sample. The assumption of LTE does not necessarily lead to errors in the derived abundances. Dufton (1993) has noted, for example, that non-LTE analyses of the B star τ Sco (Becker & Butler 1988, 1989, Becker 1991) arrived at the same elemental abundances as those obtained nearly half a century earlier by less sophisticated means (e.g. Unsöld 1942).

A sequence of low-g model atmospheres was constructed for $T_{\rm eff}$ between 14 000 and 19 000 K, with $\log g \sim 2.0 + 0.2 \times (T_{\rm eff} - 16\,000)/1\,000$, supplemented by a grid of higher gravity models at the same temperatures. At the lowest effective temperatures, these models constitute the lowest gravity models which could be calculated. On the basis of our preliminary analysis, the chemical composition was given by hydrogen and carbon abundances, $n_{\rm H} = 0.0001$, $n_{\rm C} = 0.003$ by number, solar abundances for other metals, and helium making up the residue. In the event, a second grid with $n_{\rm C} = 0.01$ was also constructed.

4. Spectrum synthesis

It was intended that the spectral analysis methods adopted should follow closely the line-by-line analysis of LSE 78 described by Jeffery (1993). However two major obstacles were encountered. First, the stars in the present sample are sufficiently cool that lines due to twice-ionized atoms of carbon, nitrogen and sulphur are weak and difficult to measure from the current spectra, excluding the possibility of measuring the ionization equilibria for these species. Second, at low surface gravities, the ionization equilibria previously used become insensitive to effective temperature, and approach the locus in $g - T_{\rm eff}$ space defined by the neutral helium line profiles. Previously, the intersection of these two loci were used to fix the stellar parameters. Therefore new procedures were developed based on the synthesis of large sections of spectrum, which can now be carried out routinely, and which reduce errors associated with the selection, measurement and analysis of individual absorption lines.

The spectral synthesis is carried out using an improved version of the radiative transfer code SPECTRUM (Dufton, Lennon, Conlon & Jeffery, unpublished). This code reads a converged model atmosphere structure, such as that computed using STERNE, and integrates the source function to obtain the emergent flux at given frequency points. The source function is computed either by assuming a strict LTE approximation ($S_\nu = B_\nu$) or by including electron scattering in which case the formal solution of the transfer equation $S_\nu = (1-\rho)B_\nu + \rho J_\nu$ is obtained using Feautrier's method. In this study, electron scattering is always included. The continuum opacity sources are matched to those used in the calculation of the model atmosphere. The ion populations assume LTE and partition functions from Traving et al. (1966). Line opacities are calculated using atomic data, including wavelengths, oscillator strengths, electron and radiative collision lifetimes and excitation potentials, taken from the CCP7 atomic data utility LTE_LINES (Jeffery 1994), which is updated from time to time to reflect the best atomic data available for the analysis of B-type stars. Classical lifetimes are used when better data are not available. Thermal and Doppler broadening is included in the Voigt profile for each line. Pretabulated broadening data are used for selected neutral helium lines (Barnard et al. 1969, Shamey 1969, Barnard et al. 1974, 1975, Dimitrijevic & Sahal Bechot 1984). More recent tabulations for neutral helium (Beauchamp et al. 1997) do not include sufficiently low densities to be useful here, whilst ionized helium lines are not observed in the current spectra. Although detailed theory is used to model the hydrogen lines (Vidal et al. 1973, Lemke 1997), they are so weak in the current spectra that Stark broadening is not important.

A complete synthetic spectrum includes over 500 transitions and 11 000 wavelength points between 3850 and 4850Å. On a Digital Alphaserver 1000A/466, each synthesis takes ~ 3 minutes. Several iterations of the procedures outlined below were necessary, involving the calculation of over 40 model atmospheres and 600 synthetic spectra.

5. Photospheric parameters and abundances

The object of analysing the spectra of the program stars is to deduce the effective temperature, surface gravity, microturbulent velocity, rotational velocity and photospheric abundances. These are evaluated by establishing equilibria for successive ionization stages of selected atoms, by fitting the profiles of Stark-broadened neutral helium lines, by constraining the abundance derived from each line of a given ion to be independent of its equivalent width, and by fitting individual line profiles. It was clear from attempts to follow previous practise that the surface gravities of all three programme stars were very low and that the effective temperatures were $14\,000 \lesssim T_{\rm eff}/K \lesssim 19\,000$.

Microturbulent and radial velocities were determined from O II lines. Synthetic spectra for O II were computed on a grid of oxygen abundances, microturbulent and rotational veloci-

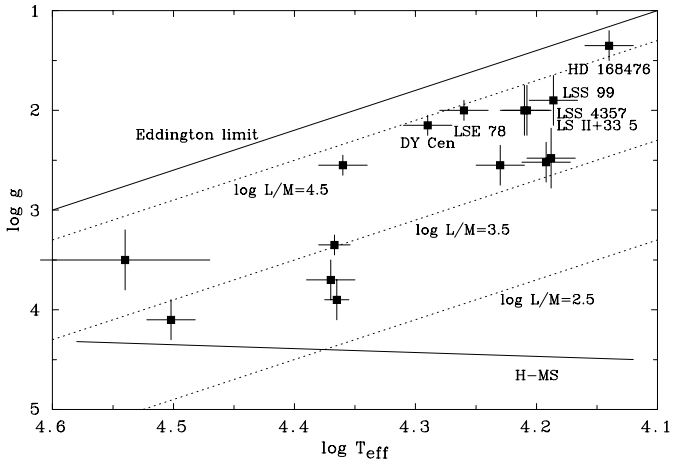

Fig. 2. The $\log g - \log\ T_{\rm eff}$ diagram for extreme helium stars showing the position of the programme stars, the hydrogen main sequence (H-MS), the classical Eddington limit for radiative stability, and loci of constant L/M (solar units: dotted lines). Other EHes referred to by name in the text are also labelled.

ties ($v \sin i$). The mean-square differences between observed and synthetic spectra were formed to establish, approximately, the oxygen abundance and more precisely the microturbulent and rotational velocities for each star (Table 1). The minima in the mean-square difference surfaces are shallow, and errors of $\pm 10 - 20\%$ are indicated. The microturbulent velocities of $\sim$ 15km/s are 50% higer than the sound speed in the line-forming region (10 km/s). As in previous studies (e.g. Drilling et al. 1998), this is a reminder that the notion of microturbulnece is useful in accounting for well-known discrepancies between theoretical and observed stellar atmospheres, but has a limited physical significance.

From this point it was possible to refine individual stellar parameters by selecting appropriate diagnostics and carrying out a mean-square residual minimization, operated as follows. In most cases, a limited grid of synthetic spectra is calculated. The difference between the observed and synthetic spectrum, normalized and velocity-shifted as described, is constructed. Where appropriate, this difference spectrum may be edited to remove unwanted information. For example, only regions of spectrum containing silicon lines would be retained to evaluate the silicon ionization equilibrium. The mean square residual is then calculated. Comparing this residual for several synthetic spectra from the grid enables a local minimum to be established. Since the location of this minimum depends on several quantities (e.g.rotation velocity, microturbulence, carbon abundance in the model grid), it is often necessary to repeat each derivation until a fully self-consistent solution is achieved.

To measure effective temperatures and surface gravities a synthetic spectrum was calculated for each model atmosphere in the grid over the interval 3900–4800 Å. A surface defined by the mean square residual with respect to the observed spectra was constructed, and a global miniumum located. In practise this minimum was constrained by the lowest gravity for which model atmospheres could be constructed. With a grid interval of 1 000 K, the effective temperature is accurate to within 500 K for a given surface gravity. However a 0.2 dex reduction in gravity could reduce the effective temperature by up to 1 000 K, with severe consequences for the remainder of the analysis. The results are given in Table 1.

The effective temperatures may in principle be cross-checked by comparing the observed ultraviolet and optical flux distribution for each star with that predicted by the model atmosphere. However previous studies have shown that this procedure gives, principally, a measurement of interstellar reddening as a function of $T_{\rm eff}$ and adds nothing to the measurement obtained from the optical spectrum.

The gravities indicate luminosity to mass ratios for the programme stars $\log L/M \sim 4.2$ (solar units), substantially lower than the critical value of 4.6 above which Heber et al. (1986) suggested that the assumption of plane-parallel geometry might be doubtful.

Once a model atmosphere has been adopted for each star, appropriate to the parameters determined in the previous section, the abundances of individual species were determined by minimizing the mean square residuals, as before, to obtain the results presented in Table 2.

Errors in photospheric abundances were previously obtained from the variance in line abundances. With synthesis methods, confidence is provided by the shape of the minima obtained in the fitting procedure. For species with many lines, a ± 0.3 dex abundance change leads to an increase in the fit statistic by $\sim$ 1%. To be more specific, especially for species with few lines, the statistic will have to be refined to exclude invariant fluxes from the fit. However, the figure of ± 0.3 dex is comparable with random errors obtained in previous line-by-line analyses. Systematic errors are discussed in detail by Drilling et al. (1998). The most important source of error here arises from the poor constraint on surface gravity, and hence on effective temperature.

In local spectral regions and considering the S/N ratio in the original spectra, a comparison between the observed and final synthetic spectra are highly satisfactory (Fig. 1). Principally because of calibration errors already described, a global comparison between the observed and synthetic spectra is less auspicious – especially in the vicinity of diffuse helium lines.

Several comments are appropriate. The calcium abundance is measured from the H and K lines. Care was taken to remove the interstellar component before fitting the line profiles. Several lines were used to measure the magnesium abundance, and not just Mg II λ4482 Å. The iron abundance measurement was unsatisfactory, being due to three Fe III$_4$ lines for which we have little confidence in the current atomic data. Consequently, in comparing the overall abundance patterns in Table 2 we have adopted a value $[\mathrm{Fe}] = -0.3$ which is more consistent with the argon and calcium measurements.

In the spectral region shown (Fig. 1), the following features attract remark. First, the diffuse singlet He I λ4388 Å and the majority of lines in this region of the spectrum are reproduced well in all three cases. For individual line identifications, the atlas by Leuenhagen et al. (1994) should be consulted. Second,

a few lines are either too strong or too weak in the model. Since the abundance for each atomic species is defined in most cases by a large ensemble of absorption lines, this probably indicates local errors in the atomic data or contamination by photon shot noise. It is noted that line-by-line analyses have yielded total variations of over 2 dex in the abundance of some species (e.g. O II in LSE 78: Jeffery 1993). One example of poor atomic data in the present case may be for C II λ4368.3 Å, which was also rejected as an abundance indicator in a recent analysis of helium star LSS 3184 (Drilling et al. 1998). Finally, a few lines simply do not appear in the model, either because reliable atomic data is not available or because they have not yet been identified. A good example is a line at 4329.9Å, also recognised but unidentified in the spectra of helium stars DY Cen, LSE 78, V348 Sgr, BD+10°2179 (Leuenhagen et al. 1994) and LSS 3184 (Drilling et al. 1998).

6. Conclusions

A quantitative analysis has provided photospheric parameters and abundances for three extreme helium stars. These have been confirmed to have effective temperatures of around 16 000 K and surface gravities close to the limit at which model atmospheres can currently be calculated in hydrostatic and local thermodynamic equilibrium. From Tables 1 and 2 and Fig. 1 it may be seen that all three stars have very similar properties. Indeed, LSS 4357 and LS II+33°5 are almost twins. No other pair of helium stars studied to date are so similar. They also have the highest oxygen abundance of any extreme helium star, previously the low-gravity helium stars DY Cen and LSE 78 held this record. In the $\log g$-$T_{\rm eff}$ diagram (Fig. 2), the programme stars lie directly between these stars and HD 168476 (Walker & Schönberner 1981), itself a moderately oxygen rich star. Together with BD$-9°4395$ (Jeffery & Heber 1992), these seven stars form a clear sequence of extreme helium stars with a luminosity to mass ratio $L/M \sim 3 \times 10^4$ (solar units). The significance of this sequence and why it appears to be distinct from a number of helium stars with $L/M \lesssim 3 \times 10^3$, will be explored in a concluding paper.

Acknowledgements. The author is indebted to Prof. U.Heber for his encouragement and for making available the observations used in this study. The computer programs and data used have been made available through the UK PPARC's Collaborative Computational Project No. 7. Software and computers provided by STARLINK have also been used. Peter Hamill and Sandra Jeffers acknowledge the Armagh Observatory for funding through the summer studentship programme. Financial support from DENI is gratefully acknowledged.

Appendix: continuum renormalization

A procedure is described for the renormalization of échelle spectra in which the blaze function has been incorrectly removed. It is not valid for spectra in which the noise level is comparable to the strength of the line spectrum. The procedure follows the following steps.

1. The original spectrum $S(x)$ is cleaned such that $a_1 < S'(x) < b_1$, rejecting all x-values with $a_1 > S(x) > b_1$.
2. A spectrum $S''(x)$ is constructed in which all the data gaps are replaced by the mean value $< S'(x) >$.
3. $S''(x)$ is smoothed using a Gaussian filter (σ) to define a pseudo-continuum $C''(x)$.
4. $S(x)$ is re-normalized using this pseudo-continuum to obtain $S_1(x) = S(x)/C''(x)$.
5. Step 1 is repeated with $a_2 < S'_1(x) < b_2$, where $b_2 - a_2 < b_1 - a_1$. This defines a more restricted set of x-values for which S(x) are more likely to be 'true' continuum values.
6. The spectrum $S''_1(x)$ is constructed in which the data gaps are replaced by the mean value $< S'(x) >$.
7. This is multiplied by the pseudo-continuum $C''(x)$ to restore valid values of $S''_1(x)$ to their original values, $S(x)$, giving $S'''_1(x) = S(x)$ with non-continuum points now replaced by a local mean rather than a global mean.
8. An improved pseudo-continuum is defined as in step 3, to give $C(x)$.
9. The renormalized spectrum is then computed from $N(x) = S(x)/C(x)$.

Steps 5 - 9 may be repeated with a decreasing interval $b - a$ until a satisfactory result is obtained. For the current CASPEC data, with R 15,000 and S/N 30, the values $a_1 = 0.95, b_1 = 1.05, a_2 = 0.98, b_2 = 1.04$ and $\sigma = 5$, the above procedure was satisfactory without further repetition.

The normalized spectrum obtained by this procedure improved the goodness-of-fit statistics considerably, but was ineffective in regions where the original continuum was incorrectly defined and where the spectrum was extremely crowded. With considerable trepidation, a second renormalization procedure was introduced, but only after the majority of the stellar parameters had been well established. In this case the following steps were taken.

1. The renormalized spectrum $N(x)$ was divided by the best available synthetic spectrum $T(x)$.
2. The result was cleaned in the same manner as before and smoothed with a Gaussian filter to define a new pseudo-continuum $C_2(x)$.
3. A completely renormalized spectrum is generated from $F(x) = N(x)/C_2(x)$.

It should be noted that throughout these procedures the equivalent widths of all absorption lines measured relative to a local continuum are not altered. The object of this renormalization is to ensure that this local continuum is normalized to unity throughout the spectrum. The final step uses information from absorption lines whose properties have already been deduced to correct regions of spectrum which may contain information (e.g. as blended lines) that cannot be recovered by other means.

References

Anderson L., Grigsby J.A., 1991, In: Crivellari L., Hubeny I., Hummer D.G. (eds.) Stellar Atmospheres: Beyond Classical Models. NATO ASI Series C, Kluwer, p.365
Asplund M., 1997, PhD Thesis, Univ. Uppsala
Avrett E.H., Loeser, 1963, JQSRT 201, 3
Barnard A.J., Cooper J., Shamey L.J., 1969, A&A 1, 28

Barnard A.J., Cooper J., Smith E.W., 1974, JQSRT 14, 1025
Barnard A.J., Cooper J., Smith E.W., 1975, JQSRT 15, 429
Beauchamp A., Wesemael F., Bergeron P., 1997, ApJS 108, 559
Becker S.R., 1991, Ph.D. Thesis, Univ. München.
Becker S.R., Butler K., 1988, A&A 201, 232
Becker S.R., Butler K., 1989, A&A 209, 244
Blöcker T., Schönberner D., 1997, A&A 324, 991
Dimitrijevic M.S., Sahal-Brechot S., 1984, 136, 289
Drilling J.S., Hill P.W., 1986, In: Hunger K., Schönberner D., Rao N.K. (eds.) Hydrogen-deficient stars and related objects. IAU Coll. 87, Reidel, Dordrecht, 499
Drilling J.S., Jeffery C.S., Heber U., 1998, A&A 329, 1019
Dufton P.L., 1993,In: Heber U., Jeffery C.S. (eds.) The Atmospheres of Early-Type Stars. Springer-Verlag, 3
Dudley R.E., Jeffery C.S., 1993, MNRAS 262, 945
Feautrier P., 1964, C. R. Acad. Sci. Paris 258, 3189
Grevesse N., Noels A., Sauval A.J., 1996, In: Holt S.S., Sonneborn G. (eds.) Cosmic abundances. ASP Conf Ser. 99, 117
Heber U., 1983, A&A 118, 39
Heber U., Jonas G., Drilling J.S., 1986, In: HungerK., Schönberner D., Rao N.K. (eds.) Hydrogen-deficient stars and related objects. IAU Coll. 87, Reidel, Dordrecht, 67
Iben I. Jr., Kaler J.B., Truran J.W., Renzini A., 1983, ApJ 264, 605
Iben I. Jr., Tutukov A., 1985, ApJS 58, 661
Jeffery C.S., 1993, A&A 279, 188
Jeffery C.S., 1994, Newsletter on 'Analysis of Astronomical Spectra' No. 16, p.17
Jeffery C.S., 1996, In: Jeffery C.S., Heber U. (eds.) Hydrogen Deficient Stars. ASP Conf Ser. 96, 152
Jeffery C.S., Heber U., 1992, A&A 260, 133
Jeffery C.S., Heber U., 1993, A&A 270, 167
Lambert D.L., Rao N.K., Gustafsson B., Asplund M., 1997, A&A submitted
Lemke M., 1997, A&AS 122, 285
Leuenhagen, U., Heber U., Jeffery C.S., 1994, A&AS 103, 445
Lucy L., 1964, SAO Special Report No. 167, p.93
Mihalas D., 1978, Stellar Atmospheres 2nd ed., Freeman, New York
Möller R.U., 1990, Diplom. Thesis, Universität Kiel
Ng K.C., 1974, J.Chem.Phys. 61, 2680
Rauch T., 1996, In: Jeffery C.S., Heber U. (eds.) Hydrogen Deficient Stars. ASP Conf Ser. 96, 174
Schmid-Burgk J., Scholz M., 1975, A&A 41, 41
Shamey L.J., 1969, PhD Thesis, Univ. Colorado
Traving G., Baschek B., Holweger H., 1966, Abh. aus der Bergedorfer Sternwarte 8, 3
Unsöld A., 1942, Zeit f. Astrophys. 21, 22
Vidal C.R., Cooper J., Smith E.W., 1973, ApJS 25, 37
Vijapurkar J., Drilling J.S., 1993, ApJS 82, 293
Walker H.J., Schönberner D., 1981, A&A 97, 291
Webbink R.F., 1984, ApJ 277, 355